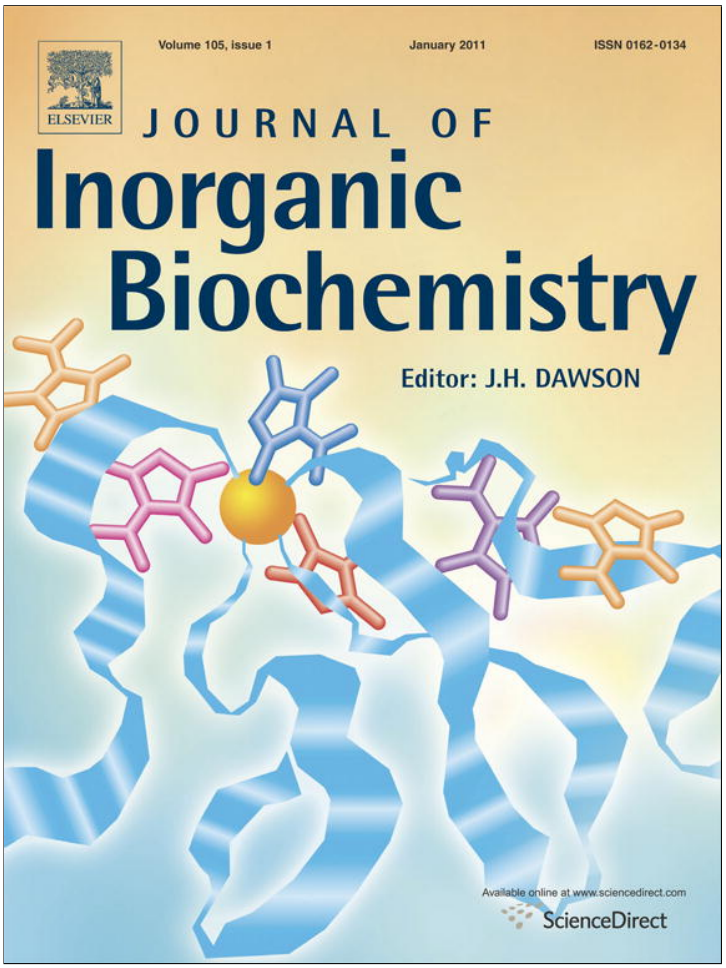

(This is a sample cover image for this issue. The actual cover is not yet available at this time.)

Journal of Inorganic Biochemistry 106 (2012) 117–125

Contents lists available at SciVerse ScienceDirect

Journal of Inorganic Biochemistry

journal homepage: www.elsevier.com/locate/jinorgbio

Synthesis, crystal structures, and biological evaluation of Cu(II) and Zn(II) complexes of 2-benzoylpyridine Schiff bases derived from S-methyl- and S-phenyldithiocarbazates

Ming Xue Li [a,b], Li Zhi Zhang [a], Chun Ling Chen [a], Jing Yang Niu [a,*], Bian Sheng Ji [b]

[a] Institute of Molecular and Crystal Engineering, College of Chemistry and Chemical Engineering, Henan University, Kaifeng 475004, PR China
[b] Key Laboratory of Natural Medicines and Immune Engineering, Henan University, Kaifeng 475004, PR China

ARTICLE INFO

Article history:
Received 16 July 2011
Received in revised form 6 September 2011
Accepted 29 September 2011
Available online 5 October 2011

Keywords:
2-benzoylpyridine
S-methyl- and S-phenyldithiocarbazates
Crystal structure
Cytotoxicity
MMP

ABSTRACT

Two NNS tridentate Schiff base ligands of 2-benzoylpyridine S-methyldithiocarbazate (HL^1) and 2-benzoylpyridine S-phenyldithiocarbazate (HL^2) and their transition metal complexes $[Cu_2(L^1)_2(CH_3COO)](ClO_4)$ (**1**), $[Zn_2(L^1)_2(ClO_4)_2]$ (**2**), $[Zn(L^2)_2]$(**3**) have been prepared and characterized by elemental analysis, IR, MS, NMR and single-crystal X-ray diffraction studies. In the solid state, each of two Schiff bases remains in its thione tautomeric form with the thione sulfur atom trans to the azomethine nitrogen atom. Under similar prepared conditions, three new complexes showed distinctly different coordination modes depending on their coordinating preferences. Each copper atom in S-bridged dinuclear complex $[Cu_2(L^1)_2(CH_3COO)](ClO_4)$ (**1**) is surrounded by five donor atoms in a square-pyramidal fashion (4 + 1). $[Zn_2(L^1)_2(ClO_4)_2]$ (**2**) is a dimer in which each zinc atom adopts a seven-coordinate distorted pentagonal bipyramidal geometry, while mononuclear $[Zn(L^2)_2]$ (**3**) has octahedral coordination geometry. Biological studies, carried out *in vitro* against selected bacteria, fungi, and K562 leukaemia cell line, respectively, have shown that different substituted groups attached at the dithiocarbazate moieties and metals showed distinctive differences in the biological property. Zinc(II) complexes **2** and **3** could distinguish K562 leukaemia cell line from normal hepatocyte QSG7701 cell line. Effect of the title compounds on Mitochondria membrane potential (MMP) and PI-associated fluorescence intensity in K562 leukaemia cell line are also studied. The title compounds may exert their cytotoxicity activity via induced loss of MMP.

1. Introduction

Sulfur–nitrogen chelating agents derived from S-alkyl/aryl esters of dithiocarbazic acid are of particular importance due to varied coordination environments which determine a variety of possible conformations and marked biological activities [1-3]. In many cases, the biological properties of S-alkyl/aryl dithiocarbazate are often related to the donor sequence of the ligands with different substituted dithiocarbazate esters showing widely different biological activities, although they may vary only slightly in their molecular structure. In addition, biological activities of the metal complexes differ from those of either the ligand or the metal ion itself, and increased and/or decreased biological activities are reported for several transition metal complexes such as copper(II) and cobalt(II) [4, 5].

Copper complexes, which are stable and relatively lipophilic, represent a class of compounds that have recently been the subject of intense research because of their potential as radiopharmaceuticals for the specific targeting of hypoxic tissue [6], as new, effective drugs for treatment of refractory neuroblastoma in children [7]. On the other hand, the zinc(II) complexes are important. Intracellular distribution of several zinc(II) complexes have been tracked in different cancer cell lines [8]. In particular, copper(II) and zinc(II) complexes are well-known for their significant pharmaceutical properties [9-11] and in most cases were found to be generally more active than their free ligands [12, 13]. Thus, knowledge of the biological evaluation of these complexes is crucial to develop new antimicrobial agents and cytotoxic agents.

In recent years we have been working on the structural and biological properties of heterocyclic thiosemicarbazones and their transition metal complexes [14-18]. These results reveal that thiosemicarbazones derived from 2-benzoylpyridine and their transition metal complexes show significant cytotoxic activities. After a careful literature search, we can affirm that the coordination chemistry and pharmacological studies of 2-benzoylpyridine dithiocarbazonates are scarce. Therefore, it seemed important for us to combine copper/zinc with 2-benzoylpyridine dithiocarbazonates and evaluate their coordination chemistry and their potential as anti-microbial and anti-cancer agents.

* Corresponding author. Tel./fax: +86 378 3886876.
E-mail addresses: jyniu@henu.edu.cn, limingxue@henu.edu.cn (J.Y. Niu).

0162-0134/$ – see front matter © 2011 Elsevier Inc. All rights reserved.
doi:10.1016/j.jinorgbio.2011.09.034

In the present work, with the main aim of comparison, we have tested the biological activity of 2-benzoylpyridine S-methyldithiocarbazate HL^1, 2-benzoylpyridine S-phenyldithiocarbazate HL^2 (Scheme 1), and their transition metal complexes formulated as $[Cu_2(L^1)_2(CH_3COO)](ClO_4)$ (**1**), $[Zn_2(L^1)_2(ClO_4)_2]$ (**2**), $[Zn(L^2)_2]$ (**3**) against bacteria, fungi, and K562 leukemic cell line, respectively. Our objective is to compare the variation in biological activity by changing different substituted groups attached at the dithiocarbazate moieties and metals. To explore their biochemical mechanism of cytotoxicity initially, effect of the title compounds on Mitochondria membrane potential (MMP) and Propidine iodide (PI)-associated fluorescence intensity in K562 leukaemia cell line are studied. In addition, we also describe the synthesis, characterization and single crystal X-ray crystal structures of the title compounds here.

2. Material and methods

2.1. General techniques and apparatus

All solvents and reagents are commercially available and were used without further purification. Elemental analysis of C, H and N was performed with a Perkin-Elmer 240 analyzer. The infrared spectra were recorded from KBr discs with a Nicolet 170 FT infrared spectrophotometer. The mass spectra were carried out on an Esquire 3000 LC-MS mass spectrophotometer. Melting points were determined with a X-5 Micro Processor Melting-point Apparatus. ^1H and ^{13}C NMR spectra were recorded in DMSO–d_6 using a BrukerAV-400 spectrometer.

2.2. Synthesis

2.2.1. Synthesis of HL^1

An ethanol solution (15 mL) containing 2-benzoylpyridine (0.73 g, 4.0 mmol) was added dropwise to an ethanol solution (20 mL) of S-methyldithiocarbazate (0.49 g, 4.0 mmol) with five drops of acetic acid as catalyst. After refluxed for 2 h, the resultant solution was filtered. Products separated were recrystallised from hot ethanol and dried over P_4O_{10} in vacuo. Yield, 81%. M.p. 113−114°C. Anal. calcd for $C_{14}H_{13}N_3S_2$ (%): C, 58.46; H, 4.52; N, 14.61. Found C, 58.53; H, 4.60; N, 14.41. ^1H NMR (DMSO-d_6, δppm): 8.86 (s, 1H, NH), 8.02(s, 1H), 7.63(s, 1H), 7.55–7.42 (m, 6H), 7.30 (s, 1H), 2.53 (s, 3H). ^{13}C NMR (DMSO-d_6, δ ppm): 200.8, 151.4, 149.6, 147.2, 138.8, 136.8, 130.3, 129.6, 129.0, 127.0, 125.8, 17.34. ESI-MS (*m*/*z*): 288.2 = $[HL^1 + H^+]$, calc. mass = 288.1. Yellow crystals suitable for X-ray studies were obtained by slow evaporation of its ethanol solution.

2.2.2. Synthesis of HL^2

HL^2 was prepared by a similar procedure to that of HL^1 using S-phenyldithiocarbazate in place of S-methyldithiocarbazate. Yield, 76%. M.p. 176−177°C. Anal. calcd for $C_{20}H_{17}N_3S_2$ (%): C, 66.03; H, 4.68; N, 11.55. Found C, 66.10; H, 4.75; N, 11.36. ^1H NMR (DMSO-d_6, δ ppm): 8.86 (s, 1H, NH), 8.05(s, 1H), 7.62(s, 1H), 7.50−7.41(m, 6H), 7.33−7.26(m, 6H), 4.49(s, 2H). ^{13}C NMR (DMSO-d_6, δ ppm): 198.8, 151.3, 149.6, 147.7, 138.78, 136.96, 136.71, 130.34, 129.72, 129.18, 129.04, 128.95, 127.74, 127.02, 125.86, 38.14. ESI-MS (*m*/*z*): 386.1 = $[HL^2 + Na^+]$, calc. mass = 386.1. Yellow crystals suitable for X-ray studies were obtained by slow evaporation of its ethanol solution.

2.2.3. Synthesis of complex **1**

An ethanol solution (10 mL) containing $Cu(ClO_4)_2{\cdot}6H_2O$ (0.09 g, 0.25 mmol) was added to an ethanol solution (20 mL) of HL^1 (0.14 g, 0.5 mmol) and NaOAc (0.04 g, 0.5 mmol). The resulting reaction mixture was refluxed for 4 h. The solid product formed was isolated and washed with ethanol. This crude product was further recrystallized from ethanol to give green microcrystals which were filtered off and dried over P_4O_{10} in vacuo. Yield, 64%. M.p. 145−147°C. Anal. calcd for $C_{30}H_{27}ClCu_2N_6S_4O_6$ (%): C, 41.94; H, 3.15; N, 9.79. Found C, 41.99; H, 3.11; N, 9.61. ESI-MS (*m*/*z*): 757.0 = $[HL^2 + Na^+]$, calc. mass = 757.0. Green crystals suitable for X-ray studies were obtained by slow evaporation of its ethanol solution. Furthermore, in accordance with our findings, the reaction of one equivalent metal ion with one equivalent of ligand also generates the desired complex **1** indicating the 1:1 metal/ligand product formed readily.

2.2.4. Synthesis of complex **2**

Complex **2** was prepared by a similar procedure to that of complex **1** using $Zn(ClO_4)_2{\cdot}6H_2O$ in place of $Cu(ClO_4)_2{\cdot}6H_2O$. Yield, 58%. M.p. 261−263°C. Anal. calcd for $C_{28}H_{24}Cl_2Zn_2N_6S_4O_8$ (%): C, 37.23; H, 2.66; N, 9.31. Found C, 37.29; H, 2.64; N, 9.08. ESI-MS (*m*/*z*): 988.9 = $[Zn_2(HL^1)\ (L^1)(ClO_4)_2(H_2O)_5]^+$, calc. mass = 988.9. Yellow crystals suitable for X-ray studies were obtained by slow evaporation of its ethanol solution.

2.2.5. Synthesis of complex **3**

Complex **3** was prepared by a similar procedure to that of complex **2** using 2-benzoylpyridine S-phenyldithiocarbazate in place of 2-benzoylpyridine S-methyldithiocarbazate. Yield, 62%. M.p. 211−213°C. Anal. calcd for $C_{40}H_{32}ZnN_6S_4$ (%): C, 60.73; H, 4.05; N, 10.63. Found C, 60.81; H, 4.01; N, 10.44. ESI-MS (*m*/*z*): 789.2 = $[Zn(L^2)(HL^2)]^+$, calc. mass = 789.1. Yellow crystals suitable for X-ray studies were obtained by slow evaporation of its ethanol solution.

2.3. X-ray crystallography

Crystallographic data were collected with a Siemens SMART-CCD diffractometer with graphite-monochromated Mo*K*α radiation (λ = 0.71073 Å). The structure were solved by Direct Methods and refined by full-matrix least-squares on F^2 with anisotropic displacement

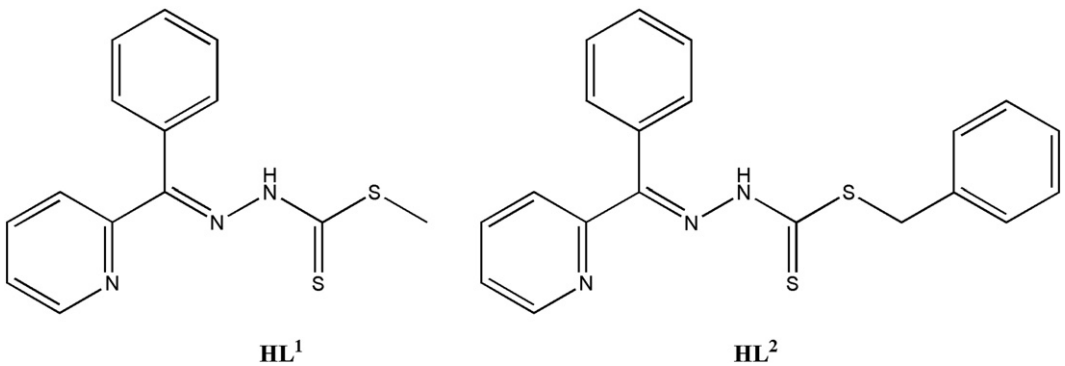

HL^1 **HL^2**

Scheme 1. Dithiocarbazates ligands (HL^1 and HL^2).

Table 1
Summary of crystal data and refinement results for HL^1, HL^2 and complexes **1**−**3**.

Crystal Data	HL^1	HL^2	**1**	**2**	**3**
Formula	$C_{14}H_{13}N_3S_2$	$C_{20}H_{17}N_3S_2$	$C_{30}H_{27}ClCu_2N_6S_4O_6$	$C_{28}H_{24}Cl_2Zn_2N_6S_4O_8$	$C_{40}H_{32}ZnN_6S_4$
Formula weight	287.39	363.49	858.35	902.41	790.33
Crystal system	Monoclinic	Monoclinic	Monoclinic	Monoclinic	Monoclinic
Space group	$P2_1/n$	$P2_1/c$	$P2_1/c$	$P2_1/c$	$P2_1/c$
a/Å	12.5242(16)	12.3607(19)	12.1408(12)	10.7126(9)	14.5341(8)
b/Å	5.5115(7)	12.599(2)	24.357(3)	7.6265(7)	15.9047(9)
c/Å	20.520(3)	11.7952(19)	13.1986(13)	22.338(2)	17.2705(9)
β/°	95.440(2)	90.588(3)	116.5580(10)	103.4400(10)	94.1880(10)
Volume/Å^3	1410.1(3)	1836.9(5)	3491.1(6)	1775.1(3)	3981.6(4)
Z	4	4	4	2	4
D_{calcd}/g cm^{-3}	1.354	1.314	1.633	1.688	1.318
Crystal habit	cuboid	stick	rectangle	block	block
Crystal color	yellow	yellow	green	yellow	yellow
μ/mm^{-1}	0.366	0.297	1.586	1.794	0.863
Crystal size/mm	0.32×0.21×0.15	0.29×0.23×0.18	0.32×0.23×0.16	0.29×0.23×0.18	0.34×0.26×0.23
θ range/°	1.83−25.00	1.65–26.00	1.67–26.00	1.87–25.00	1.74–25.00
No. reflns collected	2487	3592	6863	3092	6695
Data/restrnts/params	1915/0/173	2240/0/226	5198/34/442	2527/40/227	5327/0/460
GOOF	0.961	1.090	1.105	1.023	0.986
R_{int}	0.0426	0.0388	0.0382	0.0393	0.0200
R_1, wR_2 ($I>2\sigma(I)$)	0.0326, 0.0821	0.0504, 0.1570	0.0507, 0.1531	0.0981, 0.3128	0.0581, 0.1921
R_1, wR_2 (all data)	0.0442, 0.0870	0.0797, 0.1648	0.0702, 0.1633	0.1083, 0.3303	0.0719, 0.2074

parameters for all non-hydrogen atoms using SHELXTL [19]. The hydrogen atoms were added in idealized geometrical positions. Table 1 summarizes crystal and refinement data for the five compounds.

2.4. Antimicrobial activity

Gram-positive, Gram-negative bacteria, moulds and yeast were used for antimicrobial studies. Gram positive bacteria: *Bacillus subtilis*, *Staphylococcus aureus*, *Agrobacterium tumefaciens*. Gram negative bacteria: *Pseudomonas aeruginosa*, *Escherichia coli*, *Salmonella typhimurium*. Moulds: *Aspergillus niger*, *Mucor mucedo, Penicillium oxalicum*. Yeast: *Candida lusitaniae*. All microorganisms were provided by China General Microbiological Culture Collection Center (CGMCC). The bacterial strains were grown in Mueller-Hinton Agar (MHA) plates at 37 °C, while the moulds and yeast were grown in Potato Dextrose Agar (PDA) and Sabouraud Dextrose Agar (SDA)media, respectively, at 28 °C. The minimal inhibitory concentrations (MIC, μg/mL) were estimated by the disk diffusion method [20]. The final concentration of all cultures in Mueller-Hinon agar (MHA) for bacteria and potato dextrose agar (PDA) and Sabouraud dextrose agar (SDA) for mould spores and yeast cells was adjusted to 10^6 CFU/mL (bacteria) or 2×10^5 CFU/mL (mould spores and yeast cells) and used for inoculation in the MIC test. Serial dilutions of the test compounds (dissolved in 10% DMSO in PBS) were prepared at concentrations of 0–2000 μg/mL. To each plate was inoculated with 0.1 mL of the prepared bacterial and fungi cultures. Similarly, each plate carried a blank disc, with medium solvent containing 10% DMSO only in the center to serve as a control, as well as control antibiotics ampicillin (Amp), streptomycin (Str), kanamycin sulfate (Kan) (for bacteria) and nystatin (Nys) (for fungi). The inoculated plates were then incubated at either 37 °C for 18–20 h (bacteria) or 28 °C for 48–96 h (fungi), respectively. The minimal inhibitory concentration (MIC) was detected as the lowest concentration of drug in plate for which no visible growth took place by macroscopic evaluation. All determinations were performed in triplicate and confirmed by three separate experiments.

Table 2
IR spectral assignments (cm^{-1}) of HL^1, HL^2 and complexes **1**−**3**.

Compounds	ν(C=N)	ν(N–N)	ν(N–H)	ν(C=S)	ν(C–S)	(py)
HL^1	1583	1119	3058	1055		607
1	1539	1163			997	622
2	1545	1155			974	641
HL^2	1585	1119	3058	1052		607
3	1542	1155			965	633

2.5. cytotoxicity assay

3-(4,5-Dimethylthiazol-2-yl)-2,5-diphenyltetrazolium bromide (MTT) assay was carried out to evaluate cytotoxicity in K562 leukaemia cell line and QSG7701 cell line. Cells were plated into 96-well plates at a cell density of 1×10^4 cells per well and allowed to grow in a CO_2 incubator. After 24 h, the medium was removed and replaced by fresh medium containing the tested compounds which were dissolved in DMSO at 0.01 M and diluted to various concentrations with phosphate-buffered saline (PBS) before the experiment, the final concentration of DMSO is lower than 1%. After 24 h incubation, cultures were incubated in 100 μL of medium with 10 μL of 5 mg/mL MTT solution for 4 h at 37 °C. The medium with MTT was removed, and 100 μL of DMSO was added to each well to dissolve the formazan. The absorbance at 570 nm was measured with microplate reader (Bio-Tek ELX800, USA). The inhibitory percentage of each compound at various concentrations was calculated, and the IC_{50} value was determined.

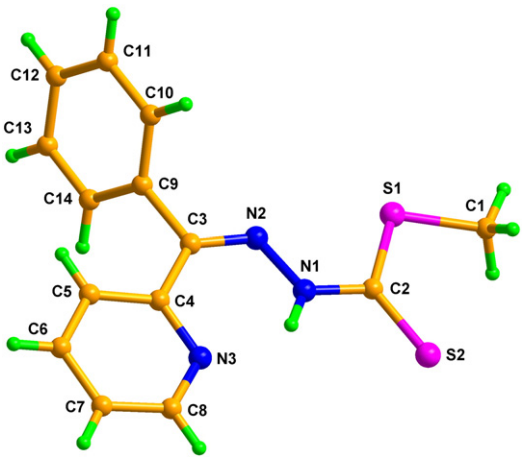

Fig. 1. Molecular structure of HL^1.

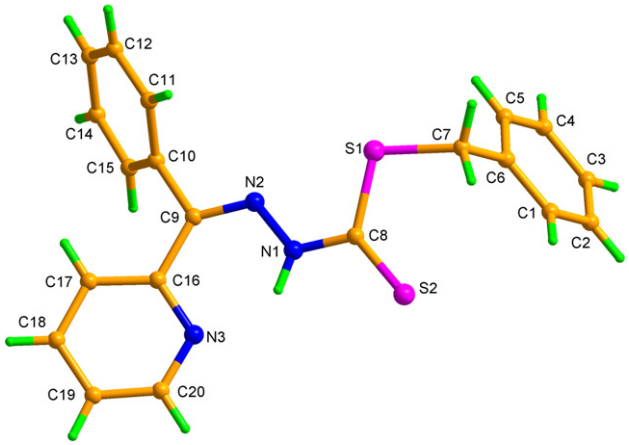

Fig. 2. Molecular structure of HL^2.

2.5.1. Measurement of mitochondrial membrane potential (MMP)

After incubation with the tested compounds with different concentration for 48 h, the K562/DOX cells were preloaded with Rhodamine 123(Rh123) (2 μM) and Hoechst 33342 (3 mg/ml) for 30 min at 37 °C, and then rinsed with freshly prepared phosphate-buffered saline (PBS). The fluorescence intensity was measured at emission wavelength of 530 nm and excitation wavelengths of 480 nm by High-Content Screening Reader (Arrary Scan VTI 600, USA).

Statistical analysis: All the data were expressed as mean ± S.D. and analyzed using analysis of variance (ANOVA) followed by Student's *t*-test. Differences were considered statistically significant at $p<0.05$.

2.5.2. PI staining

After incubation with the tested compounds with different concentration for 48 h, the K562/DOX cells were preloaded with Propidine iodide (PI)(100 μg/ml) and Hoechst 33342 (3 mg/ml) for 30 min at 37 °C, and then rinsed with freshly prepared phosphate-buffered saline (PBS). The fluorescence intensity was measured at emission wavelength of 620 nm and excitation wavelengths of 488 nm by High-Content Screening Reader (Arrary Scan VTI 600, USA).

Statistical analysis: All the data were expressed as mean ± S.D. and analyzed using analysis of variance (ANOVA) followed by Student's *t*-test. Differences were considered statistically significant at $p<0.05$.

3. Results and discussion

3.1. Spectral studies

The tentative assignments of the significant IR spectral bands of the free ligands HL^1, HL^2 and their complexes **1**−**3** are presented in Table 2. The infrared spectral bands most useful for determining the mode of coordination of the ligands are the ν(C=N), ν(N−N) and ν(C=S) vibrations. The IR spectra of HL^1 and HL^2 do not display ν(S–H) at around 2700 cm^{-1} indicating that in the solid state two ligands remain in the thione form [21]. A comparison of the IR spectra of the ligands with their complexes indicate that the ν(N–H) bands of the free ligands are not present in the spectra of the complexes, supporting deprotonation of the ligands during coordination. The shift of the ν(C=N) bands of the free ligands to lower wavenumbers and the shift of the ν(N–N) bands to higher wavenumbers in the IR spectra of the complexes support coordination of the ligands to the metal atom via the azomethine nitrogen atom [22]. The HL^1 and HL^2 showed ν(C=S) modes at 1055 and 1052 cm^{-1}, respectively. In the spectra of the complexes, the ν(C=S) modes observed disappeared and consequently the ν(C−S) modes are observed confirming that complexation occurred [23]. The breathing motion of the pyridine ring is shifted to a higher frequency upon complexation and is consistent with pyridine ring nitrogen coordination. The $\nu(ClO_4)$ bands in complexes **1** and **2** are found at 1089 and 1088 cm^{-1}, respectively. Based on the above spectral evidences, it is confirmed that the free ligand is tridentate, coordinating via pyridyl nitrogen, azomethine nitrogen and the thiolato sulfur atoms. These observations have also been confirmed by X-ray single crystal structure analysis.

3.2. X-ray crystallography

In view of the structural similarity of HL^1 and HL^2 (see Figs. 1 and 2, and Tables 3–5), only HL^1 was described in some detail. As shown in Fig. 1, in the solid state, the free ligand HL^1 remains in its thione tautomeric form (supported by the presence of hydrazinic N−H and C−S distance of 1.653(2) Å, which is much shorter than a single C−S bond) with the thione sulfur atom trans to the azomethine nitrogen atom. A comparison of the N(1)–N(2) distance of 1.372(2) Å with that in S-methyldithiocarbazate [24] shows that the bond is shorter than a single N–N bond (1.44 Å) indicating that a significant π-charge delocalization occurs along the C–N–N–C moiety. Unlike the

Table 4
Selected bond lengths (Å) and angles (°) of HL^2 and complex **3**.

HL^2		**3**	
N(2)–C(9)	1.302(4)	Zn(1)–S(2)	2.4171(1)
S(2)–C(8)	1.652(3)	Zn(1)–N(2)	2.145(3)
N(1)–N(2)	1.366(3)	Zn(1)–N(3)	2.242(3)
N(1)–C(8)	1.334(4)	S(2)–C(8)	1.715(4)
S(1)–C(7)	1.806(3)	N(2)–C(9)	1.285(5)
S(1)–C(8)	1.764(3)	S(4)–C(28)	1.721(4)
C(8)–N(1)–N(2)	120.4(2)	N(5)–Zn(1)–S(2)	114.44(9)
C(9)–N(2)–N(1)	118.4(2)	N(5)–Zn(1)–N(3)	90.26(1)
N(1)–C(8)–S(2)	121.1(2)	N(2)–Zn(1)–S(4)	119.54(9)
N(1)–C(8)–S(1)	112.2(2)	N(6)–Zn(1)–S(4)	153.58(8)

Table 3
Selected bond lengths (Å) and angles (°) of HL^1, **1** and **2**.

HL^1		1		2	
S(2)–C(2)	1.653(2)	Cu(1)–O(2)	1.930(3)	Zn(1)–O(1)	2.072(1)
N(2)–C(3)	1.300(2)	Cu(1)–N(2)	1.950(4)	Zn(1)–N(3)	2.163(6)
N(1)–N(2)	1.372 (2)	Cu(1)–N(3)	2.006(4)	Zn(1)–S(2)	2.390(2)
N(1)–C(2)	1.350(2)	Cu(1)–S(2)	2.278 (1)	Zn(1)–N(2)	2.104(6)
S(1)–C(2)	1.738(2)	S(2)–C(2)	1.749(5)	Zn(1)–O(4)	2.163(12)
S(1)–C(1)	1.796(2)	S(4)–C(16)	1.755(5)	S(2)–C(2)	1.724(7)
		N(1)–C(2)	1.293(6)	N(2)–C(3)	1.287(9)
C(2)–N(1)–N(2)	120.33(14)	O(2)–Cu(1)–S(2)	99.67(11)	O(1)–Zn(1)–N(3)	99.8(4)
C(3)–N(2)–N(1)	118.09(14)	N(3)–Cu(1)–S(2)	163.54(12)	N(3)–Zn(1)–S(2)	154.31(2)
N(1)–C(2)–S(2)	119.27(13)	O(2)–Cu(1)–N(2)	171.41(16)	N(2)–Zn(1)–O(4)	109.4(3)
N(1)–C(2)–S(1)	114.74(12)	N(2)–Cu(1)–N(3)	80.50(15)	N(2)–Zn(1)–O(1)	142.5(3)
S(2)–C(2)–S(1)	125.98(10)	N(2)–Cu(1)–S(2)	84.87(110	S(2)–Zn(1)–O(4)	97.6(4)

Table 5
Hydrogen bond lengths (Å) and bond angles (°) of HL^1 and HL^2.

	D–H…A	*d*(H…A)	*d*(D…A)	∠(DHA)
HL^1	N(1)–H(1A)–N(3)	1.95	2.634(2)	135.6
HL^2	N(1)–H(1A)–N(3)	1.97	2.650(4)	135.2

2-acetylpyrazine Schiff base of S-benzyldithiocarbazate [25], the pyridine nitrogen atom N(3) is not trans to the azomethine nitrogen atom N(2). The conformation of the molecule is mainly determined by the intramolecular hydrogen bonds between the hydrazine nitrogen atom N(1) and the pyridine nitrogen atom N(3) (N(1)—H(1)…N(3) 2.634(2) Å) (see Figs. 3 and 4, and Table 5).

The molecular structure of complex **1** contains dinuclear $[Cu_2(L^1)_2(CH_3COO)]^+$ cation in which sulfur atom bridges the two copper(II) ions (Fig. 5) and free perchlorate anion. Each of the two copper atoms in $[Cu_2(L^1)_2(CH_3COO)]^+$ adopts a five-coordinate near square-pyramidal geometry with an N_2S_2O coordination environment. The pyridine nitrogen (N(3)/(N6)), the azomethine nitrogen atom (N(2)/N(5)) and the thiolate sulfur atom (S(2)/S(4)) together with the carboxyl oxygen atom (O(2)/O(1)) from acetate group ligand comprise the basal plane of the square-pyramid whereas the thiolate sulfur atom (S(4)/S(2))of another ligand occupies the apical position. The large difference between the two Cu–S distances (Cu(1)—S(2) 2.278(1) Å/ Cu(2)—S(4) 2.264(1) Å in the basal plane and Cu(1)—S(4)2.878 Å/Cu(2)—S(2) 2.838 Å in the apical position) can be ascribed to a Jahn-Teller distortion [26]. Copper(II) dimers with such a thiolate sulfur bridging have also been observed in other dithiocarbazate copper(II) complexes [27].

The C–S bond length increases from 1.653(2) Å to 1.749(5) and 1.755(5) Å, respectively. Similarly, C(2)–N(1) suffers a significant decrease from 1.350(2) Å to 1.293(6) Å. These changes with enhanced single and double bond characters indicate the ligand in the present complex is coordinated in its deprotonated thiolate form as observed in most complexes derived from S-alkyl/aryl dithiocarbazates [28]. The two dithiocarbazate ligands have slightly different Cu–N(pyridine) bond distances and they are longer than the Cu–N(azomethine) distances, this may be attributed to the fact that the azomethine nitrogen is a stronger base compared with the pyridine nitrogen [29].

Single crystal X-ray studies show that complex **2** is a centrosymmetric dimer in which each zinc atom adopts a seven-coordinate distorted pentagonal bipyramidal geometry with an N_2SO_4 coordination environment, the Schiff base coordinating as a uninegatively charged tridentate ligand chelating through the pyridine and azomethine nitrogen atoms and the thiolate, four oxygen atoms from two perchlorate

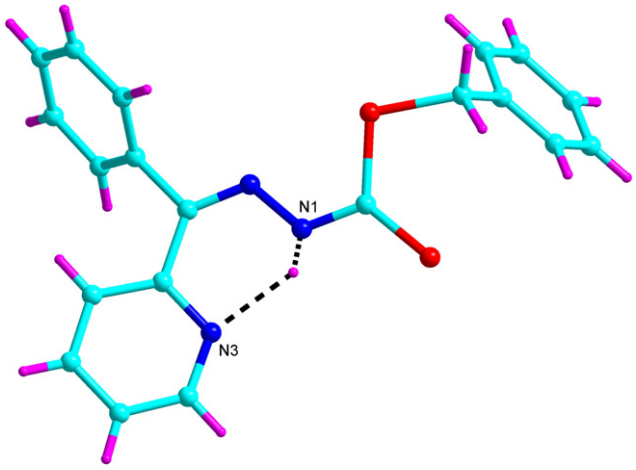

Fig. 4. Hydrogen bond in dashed lines in HL^2.

groups completing the coordination sphere (Fig. 6). Zn(II) ion usually favors tetrahedral coordination [23]. Zinc ion in complex **2** forms an irregular seven-coordinate polyhedron regarded as a special mode of bonding.

Complex **3** (Fig. 7) is a mononuclear six-coordinate complex with the basic formula $[Zn(L^2)_2]$. The octahedrally hexa coordinate Zn(II) center is coordinated in an N_4S_2 manner by two monodeprotonated ligand moieties and form four five membered chelate rings. One sulfur atom, one imine nitrogen atom and one pyridine nitrogen atom from one ligand and one imine nitrogen atom from another ligand occupy the basal positions, the two remaining positions in the octahedral geometry are the axial ones which are occupied by one sulfur atom and one pyridine nitrogen atom from the second ligand. The measured C–S bond distances ca. 1.715(4) and 1.721(4) Å are within the normal range of C–S single bonds, indicating that the dithiocarbazate moieties adopt the thiol tautomeric form and acted as a mononegative ligand.

3.3. Antimicrobial activity

Taking into account that S-alkyl/aryl esters of dithiocarbazate show antimicrobial activity [30], we have tested the ability of the title compounds against both bacteria and fungi. Based on the minimum inhibitory concentrations (Table 6), the synthesized compounds showed varying degrees of inhibition against the tested microorganisms. In general, the inhibitory activity against the

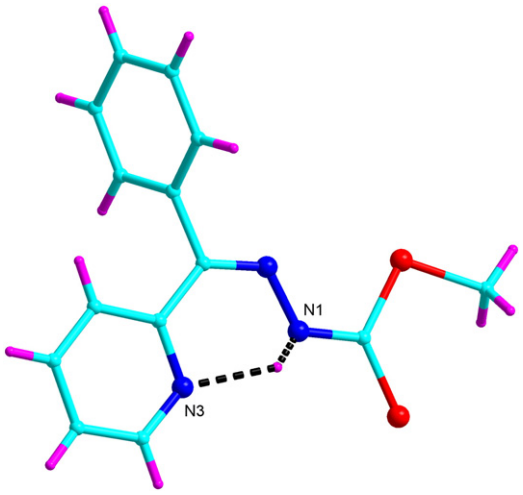

Fig. 3. Hydrogen bond in dashed lines in HL^1.

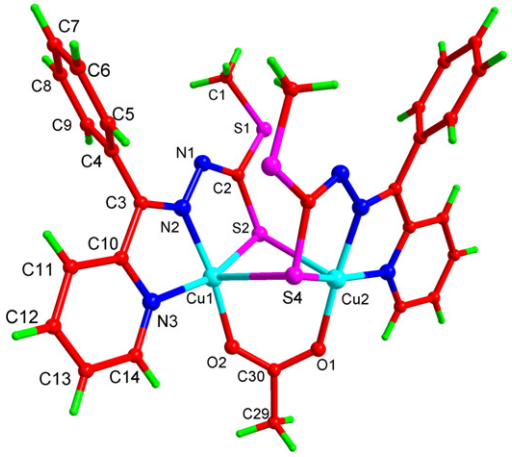

Fig. 5. Molecular structure of complex **1**.

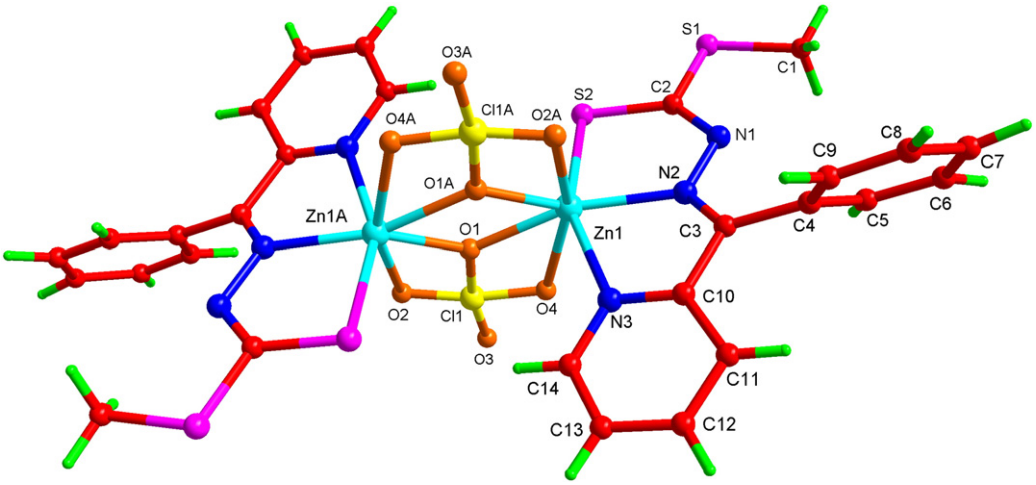

Fig. 6. Molecular structure of complex **2**.

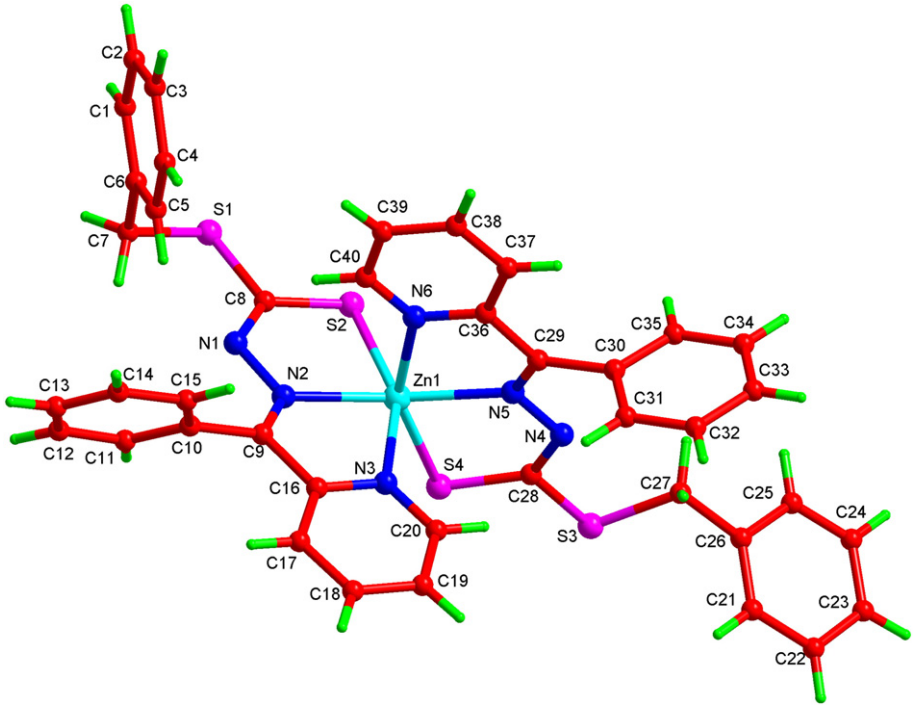

Fig. 7. Molecular structure of complex **3**.

Gram-positive bacteria was higher than that of the Gram-negative bacteria. HL^1 and **1** showed excellent activity against Gram positive bacteria *B. subtilis, S. aureus* and yeast *C. lusitaniae* with MIC values of 1—5 μg/mL. The comparison of antimicrobial activity of the free ligands indicates that 2-benzoylpyridine S-methyldithiocarbazate HL^1 is more potent than 2-benzoylpyridine S-phenyldithiocarbazate HL^2 towards the tested microorganisms, which indicate that the structure factors which govern antimicrobial activities are strongly dependent on their substitutents. And at the same time, it is clearly observed that complexation with metals has a synergetic effect on the antimicrobial activity of these compounds and the antimicrobial activity depends upon the type of metal ion. Coupling of HL^1 and HL^2 to Zn(II), respectively, decrease the antimicrobial activity of their parent ligands. As can be expected, copper(II) complex **1** results in enhanced antimicrobial activity consistent with the previously reported data [31].

Table 6
Minimal inhibitory concentration (μg/mL) of HL^1, HL^2 and complexes **1**—**3**.

	MIC (μg/mL)									
microorganisms	HL^1	**1**	**2**	HL^2	**3**	Solvent	Amp	Str	Kan	Nys
B. subtilis	1	1	100	100	125	–	5	20	10	
S. aureus	5	1	–	–	–	–	5	20	10	
A. tumefaciens	100	12.5	125	–	–	–	10	20	20	
P. aeruginosa	100	12.5	125	125	–	–	–	–	40	
E. coli	–[a]	–	–	–	–	–	5	10	20	
S. typhimurium	–	–	–	–	–	–	20	–	40	
A. niger	–	–	–	–	–	–				10
M. mucedo	100	62.5	–	–	–	–				20
P. oxalicum	–	–	–	–	–	–				10
C. lusitaniae	1	1	125	125	–	–				20

[a] No inhibition or MIC>200 μg/mL, Solvent: 10% DMSO in PBS (No inhibitory against the microorganisms).

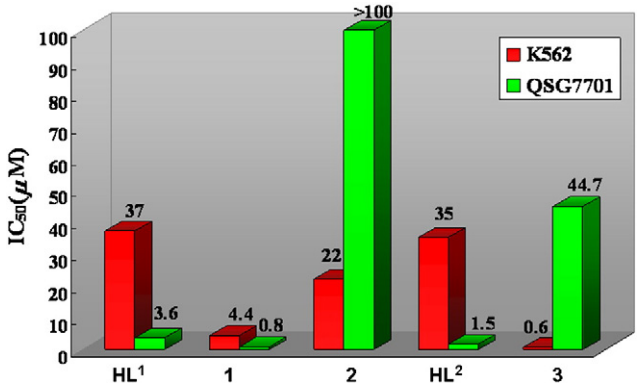

Fig. 8. The cytotoxic activities of the free ligands and the title complexes against K562 leukaemia cell line and normal hepatocyte QSG7701 cell line.

3.4. Antimour activity

In view of the cytotoxic activity of sulfur–nitrogen chelating agents [32, 33], we have tested the ability of the title ligands and their complexes to inhibit tumor cell growth against K562 leukaemia cell line. To explore the toxicity of these compounds, their effect on normal QSG7701 cell line is also described. In our experiments, IC_{50} values (compound concentration that produces 50% of cell death) in micro molar units were calculated (see Fig. 8). Although a clear structure-activity relationship cannot be deduced from the limited number of compounds investigated, several preliminary conclusions may be drawn.

As shown in Fig. 8, heterocyclic substituted dithiocarbazates and their metal complexes show particularly effective cytotoxic activity against K562 leukaemia cell line, due to the NNS tridentate system [34]. The comparison of cytotoxic activity of the free ligands and their metal complexes indicates that HL^2 shows slightly lower IC_{50} value (35 μM) than the HL^1 (37 μM), complex **3** ($IC_{50}=0.6$ μM) show remarkably higher activity than complex **2** ($IC_{50}=22$ μM), which indicate that the presence of bulky nonpolar S-substituents at dithiocarbazates moiety enhanced the cytotoxic activities very similar to the previously reported N(4)-substituted thiosemicarbazones cases [35, 36]. And at the same time, it is clearly observed that complexation with metals has a synergetic effect on the biological activity of these compounds and the biological activity depends upon the type of metal ion. As can be expected, the title Cu(II) and Zn(II) complexes increase the biological activity of their parent ligands, consistent with other copper and zinc compounds [37, 38]. This confirms the conclusion that the cytotoxic activities of Schiff base can be enhanced by coordinating the ligand to Cu(II) and Zn(II) cations [39]. The better activities of these metal complexes compared to their respective ligands may be due to chelation, which reduces the polarity of the central metal atom because of partial sharing of its positive charge with the ligand [40]. It should be emphasized that Zn(II) complex **3** effectively inhibit K562 leukaemia cell line at concentrations more than 61-fold lower than HL^2 and Cu(II) complex **1** effectively inhibit K562 leukaemia cell line at concentrations more than 8-fold lower than HL^1. Importantly, IC_{50} values of zinc(II) complexes 2 and 3 are obviously higher in QSG7701 cell line than in K562 leukaemia cell line, indicating both of them have tumor cells selectivity. Therefore, the complexes studied in the present work may be endowed with important cytotoxic properties and would be good candidates to be used for medical practice as metal-based drugs.

3.5. Effect of the title compounds on mitochondria membrane potential (MMP) and PI-associated fluorescence intensity in K562 leukaemia cell line

Mitochondria was considered to be a major site of cytotoxic agents through electron leakage from the electron transport chain [41, 42], the decreased MMP may open the mitochondrial permeability transition (MPT) and trigger the release of cytochrome c which activate

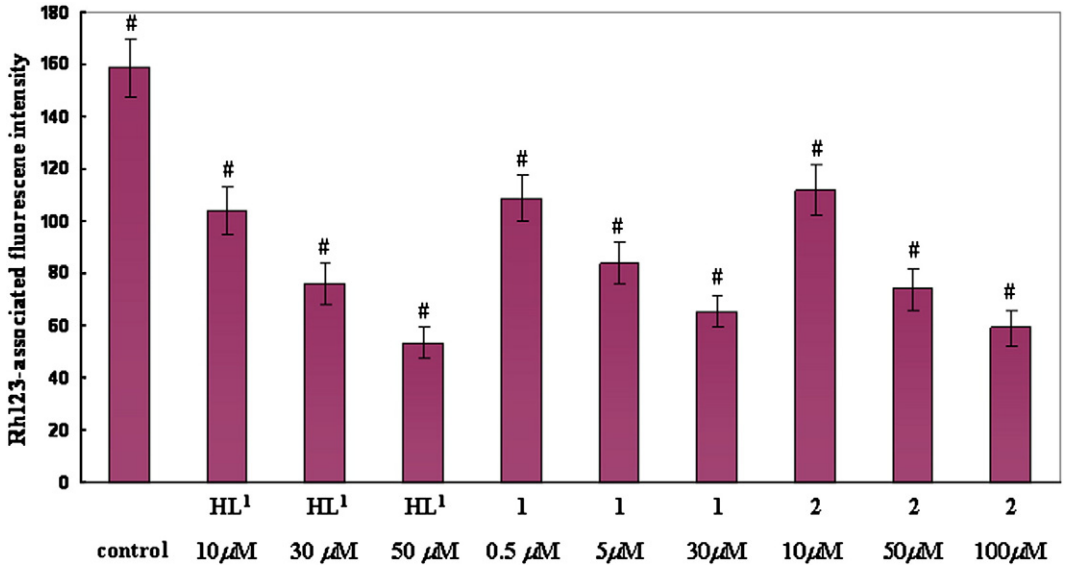

Fig. 9. Effect of HL^1, **1** and **2** on MMP in K562 leukaemia cell line. Each value represents the mean ± S.D. from four experiments. #: $p<0.05$ vs control.

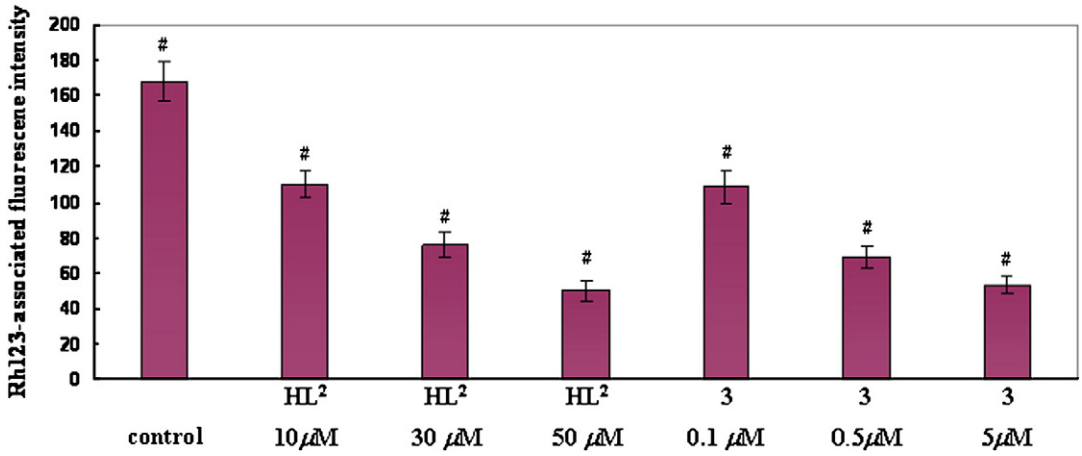

Fig. 10. Effect of $HL^2$and **3** on MMP in K562 leukaemia cell line. Each value represents the mean ± S.D. from four experiments. #: $p<0.05$ vs control.

caspase cascade, causing the cell death. In the present report, rhodamine 123 (Rh123), a mitochondrial specific stain that is dependent on the transmembrane potential, and another one, Propidine iodide (PI), were applied for the determination of MMP and apoptosis cells as well as necrosis cells, respectively. As shown in Figs. 9–12, the PI-associated fluorescence intensity in K562 leukaemia cells was increased in a concentration-dependent manner companying decreased MMP after incubation with the tested compounds for 48 h, indicating the remarkable cytotoxic activity in vitro. The present results also revealed that the complexes **1** and **3** exhibited more potent

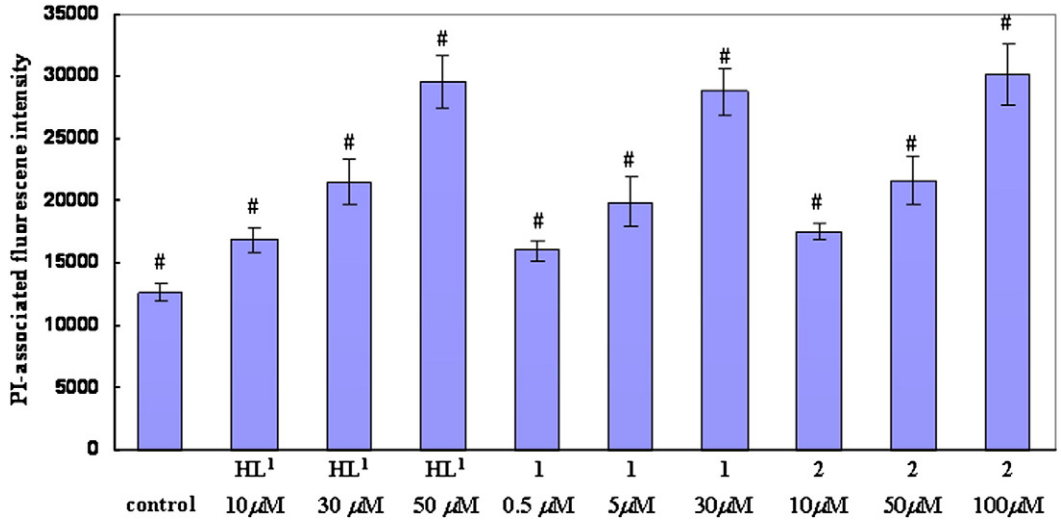

Fig. 11. Effect of HL^1, **1** and **2** on PI-associated fluorescence intensity in K562 leukaemia line. Each value represents the mean ± S.D. from four experiments. #: $p<0.05$ vs control.

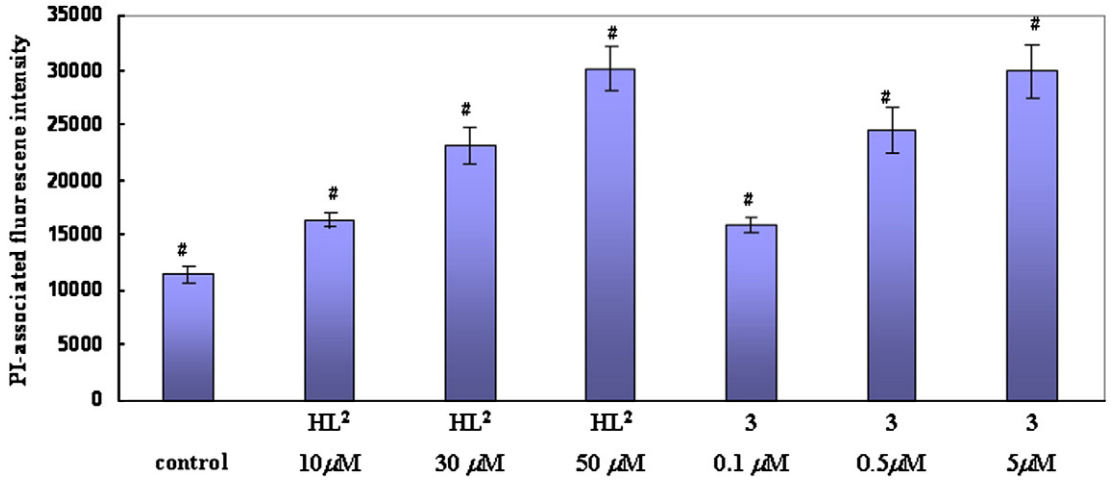

Fig. 12. Effect of HL^2 and **3** on PI-associated fluorescence intensity in K562 leukaemia line. Each value represents the mean ± S.D. from four experiments. #: $p<0.05$ vs control.

effects than their parent ligand, which was consistent with their actions in MTT assay.

Abbreviations

HL^1	2-benzoylpyridine S-methyldithiocarbazate
HL^2	2-benzoylpyridine S-phenyldithiocarbazate
MMP	Mitochondria membrane potential
DMSO-d_6	Deuterated dimethyl sulphoxide
MIC	Minimal inhibitory concentrations
DMSO	Dimethyl sulphoxide
MTT	3-(4,5-Dimethylthiazol-2-yl)-2,5-diphenyltetrazolium bromide
PBS	Phosphate-buffered saline
PI	Propidine iodide
MPT	Mitochondrial permeability transition
Rh123	Rhodamine 123

Acknowledgements

This work was financially supported by the National Natural Science Foundation of China (21071043), the China Postdoctoral Science Foundation (20090460847) and the Natural Science Foundation of the Educational Department of Henan Province (2010B150003).

References

[1] A.B. Beshir, S.K. Guchhait, J.A. Gascón, G. Fenteany, Bioorganic & Medicinal Chemistry Letters 18 (2008) 498–504.
[2] T. Bal, B. Atasever, Z. Solakoğlu, S. Erdem-Kuruca, B. Ülküseven, European Journal of Medicinal Chemistry 42 (2007) 161–167.
[3] P.K. Sasmal, A.K. Patra, A.R. Chakravarty, Journal of Inorganic Biochemistry 102 (2008) 1463–1472.
[4] M.E. Hossajn, M.N. Alam, M.A. Ali, M. Nazimuddin, F.E. Smith, R.C. Hynes, Polyhedron 15 (1996) 973–980.
[5] M.E. Hossajn, M.N. Alam, J. Begum, M.A. Ali, M. Nazimuddin, R.C. Hynes, Inorganica Chimica Acta 249 (1996) 207–213.
[6] J.P. Holland, F.I. Aigbirhio, H.M. Betts, P.D. Bonnitcha, P. Burke, M. Christlieb, G.C. Churchill, A.R. Cowley, J.R. Dilworth, P.S. Donnelly, J.C. Green, J.M. Peach, S.R. Vasudevan, J.E. Warren, Inorganic Chemistry 46 (2007) 465–485.
[7] H. Zhang, R. Thomas, D. Oupicky, F. Peng, Journal of Biological Inorganic Chemistry 13 (2008) 47–55.
[8] A.R. Cowley, J. Davis, J.R. Dilworth, P.S. Donnelly, R. Dobson, A. Nightingale, J.M. Peach, B. Shore, D. Kerr, L. Seymour, Chemical Communications (2005) 845–847.
[9] R. Ruiz, B. García, J. Garcia-Tojal, N. Busto, S. Ibeas, J.M. Leal, C. Martins, J. Gaspar, J. Borrás, R. Gil-García, M. González-Álvarez, Journal of Biological Inorganic Chemistry 15 (2010) 515–532.
[10] D. Dayal, D. Palanimuthu, S.V. Shinde, K. Somasundaram, A.G. Samuelson, Journal of Biological Inorganic Chemistry 16 (2011) 621–632.
[11] S.C. Lim, K.A. Price, S.F. Chong, B.M. Paterson, A. Caragounis, K.J. Barnham, P.J. Crouch, J.M. Peach, J.R. Dilworth, A.R. White, P.S. Donnelly, Journal of Biological Inorganic Chemistry 15 (2010) 225–235.
[12] T. Rosu, E. Pahontu, S. Pasculescu, R. Georgescu, N. Stanica, A. Curaj, A. Popescu, M. Leabu, European Journal of Medicinal Chemistry 45 (2010) 1627–1634.
[13] C.R. Kowol, R. Trondl, V.B. Arion, M.A. Jakupec, I. Lichtscheidl, B.K. Keppler, Dalton Transactions 39 (2010) 704–706.
[14] M.X. Li, C.L. Chen, C.S. Ling, J. Zhou, B.S. Ji, Y.J. Wu, J.Y. Niu, Bioorganic & Medicinal Chemistry Letters 19 (2009) 2704–2706.
[15] M.X. Li, C.L. Chen, D. Zhang, J.Y. Niu, B.S. Ji, European Journal of Medicinal Chemistry 45 (2010) 3169–3177.
[16] M.X. Li, D. Zhang, L.Z. Zhang, J.Y. Niu, Inorganic Chemistry Communications 13 (2010) 1268–1271.
[17] M.X. Li, D. Zhang, L.Z. Zhang, J.Y. Niu, B.S. Ji, Inorganic Chemistry Communications 13 (2010) 1572–1575.
[18] M.X. Li, D. Zhang, L.Z. Zhang, J.Y. Niu, B.S. Ji, Journal of Organometallic Chemistry 696 (2011) 852–858.
[19] G.M. Sheldrick, SHELXTL (Version 5.1), Bruker AXS Inc, Madison, Wisconsin (USA), 1997.
[20] S.A. Khan, K. Saleem, Z. Khan, European Journal of Medicinal Chemistry 42 (2007) 103–108.
[21] S. Singh, N. Bharti, F. Naqvi, A. Azam, European Journal of Medicinal Chemistry 39 (2004) 459–465.
[22] M.A. Ali, A.H. Mirza, M.H.S.A. Hamid, P.V. Bernhardt, O. Atchade, X. Song, G. Eng, L. May, Polyhedron 27 (2008) 977–984.
[23] M.T.H. Tarafder, K. Chew, K.A. Crouse, A.M. Ali, B.M. Yamin, H.K. Fun, Polyhedron 21 (2002) 2683–2690.
[24] S. Shanmugam, S. Raj, B.M. Yamin, Y.A. Yusof, M.T.H. Tarafder, H.K. Fun, K.A. Crouse, Acta Crystallographica C56 (2000) 1236–1237.
[25] M.A. Ali, A.H. Mirza, M.H.S.A. Hamid, P.V. Bernhardt, Polyhedron 24 (2005) 383–390.
[26] M. Baldini, M. Belicchi-Ferrari, F. Bisceglie, G. Pelosi, S. Pinelli, P. Tarasconi, Inorganic Chemistry 42 (2003) 2049–2055.
[27] J. García-Tojal, M.K. Urtiaga, R. Cortés, L. Lezama, M.I. Arriortua, T. Rojo, Journal of the Chemical Society Dalton Transactions (1994) 2233–2238.
[28] E.W. Ainscough, A.M. Brodie, J.D. Ranford, J.M. Waters, Journal of the Chemical Society Dalton Transactions (1991) 1737–1742.
[29] A. Sreekanth, M.R.P. Kurup, Polyhedron 23 (2004) 969–978.
[30] S.M.M.H. Majumder, M.A. Ali, F.E. Smith, M.A.U. Mridha, Polyhedron 7 (1988) 2183–2187.
[31] M. Joseph, M. Kuriakose, M.R.P. Kurup, E. Suresh, A. Kishore, S.G. Bhat, Polyhedron 25 (2006) 61–70.
[32] L. Thelander, A. Graslund, Journal of Biological Chemistry 258 (1983) 4063–4066.
[33] P.F. Iqbal, A.R. Bhat, A. Azam, European Journal of Medicinal Chemistry 44 (2009) 2252–2259.
[34] J.G. Tojal, A.G. Orad, J.L. Serra, J.L. Pizarro, L. Lezama, M.I. Arriortua, T. Rojo, Journal of Inorganic Biochemistry 75 (1999) 45–54.
[35] S.K. Jain, B.S. Garg, Y.K. Bhoon, Spectrochim. Acta. A42 (1986) 959–968.
[36] H. Beraldo, D. Gambino, Mini Reviews in Medicinal Chemistry 4 (2004) 159–165.
[37] M.A.H. Mirza, R.J. Butcher, M.T.H. Tarafder, T.B. Keat, A.M. Ali, Journal of Inorganic Biochemistry 92 (2002) 141–148.
[38] M. Das, S.E. Livingstone, British Journal of Cancer 37 (1978) 466–469.
[39] N. Farrell, Coordination Chemistry Reviews 232 (2002) 1–230.
[40] S. Singh, N. Bharti, P.P. Mohapatra, Chemical Reviews 109 (2009) 1900–1947.
[41] J.F. Turrens, Journal of Physiology 552 (2003) 335–344.
[42] I. Lizasoain, C.P. Weiner, R.G. Knowles, S. Moncada, Pediatric Research 39 (1996) 779–788.